DEUTSCHES ELEKTRONEN-SYNCHROTRON DESY

DESY 85-086
FTUAM-85-3
August 1985

A STUDY OF ENERGY-ENERGY CORRELATIONS WITH TASSO AND PLUTO

by

F. Barreiro
Universidad Autonoma de Madrid, 28049-Madrid, Spain
and
Universität-GH Siegen, Siegen, Germany

ISSN 0418-9833

NOTKESTRASSE 85 · 2 HAMBURG 52

To be sure that your preprints are promptly included in the
HIGH ENERGY PHYSICS INDEX ,
send them to the following address (if possible by air mail) :

DESY
Bibliothek
Notkestrasse 85
2 Hamburg 52
Germany

DESY 85-086
FTUAM-85-3
August 1985

ISSN 0418-9833

A STUDY OF ENERGY-ENERGY CORRELATIONS WITH TASSO AND PLUTO

F. Barreiro
Universidad Autónoma de Madrid
28049-Madrid, Spain

and

Universität-GH Siegen
Siegen, Germany

ABSTRACT

We present data on energy-energy correlations, EEC, at center of mass energies of 14, 22, 34 and 43 GeV. We discuss the importance of measuring the energy dependence of the related asymmetry, AEEC, as a meaningful way of determining the strong coupling constant in e^+e^- annihilation continuum. We also discuss the EEC data in the back-to-back configuration as a possible mean to test perturbative QCD at all orders.

Invited talk given at the XVI Symposium on Multiparticle Dynamics, Tel Aviv.

I) INTRODUCTION

In order to test perturbative QCD predictions in e^+e^- annihilation continuum, we have to search for quantities characterising the hadronic final states of interest, which are not only infrared finite but which are also not sensitive to [1]:

i) higher order corrections
ii) radiation of soft gluons
iii) final state interactions

With the exception of the total cross section $\sigma(e^+e^- \to \text{hadrons})$, the AEEC is the only quantity known to us so far which statisfies best these requisites. Let me discuss this in some detail.

The EEC is a measurement of the energy flow into two calorimeters subtending solid angles $d\Omega$ and $d\Omega'$. We are interested in the average EEC obtained by integrating over their orientations while keeping their relative angle χ fixed i.e.[2]

$$f(\chi) = \frac{d\Sigma}{d\cos\chi} = \frac{1}{4\sigma} \sum_{ij} \int \frac{d^3\sigma}{dx_i dx_j d\cos\chi} x_i x_j dx_i dx_j \qquad (1)$$

the sum running over all possible pairs of particles in the final state, $x_{i,j}$ denoting the energy of the ith or jth particle in units of $\frac{\sqrt{s}}{2}$ and χ being the angle between them.

It is interesting to define the forward-backward asymmetry, AEEC, i.e.

$$\frac{d\,\Sigma^A}{d\cos\chi} = f(\pi-\chi) - f(\chi) \qquad (2)$$

In the lowest non trivial order, the perturbative calculation yields[2]

$$\frac{d\,\Sigma}{d\cos\chi} = \frac{\alpha_s}{\pi} F(\chi) \qquad (3)$$

$F(\chi)$ being a function containing the angular dependence, while the energy dependence is implicit in the variation of the strong coupling constant. Then

$$\frac{d\,\Sigma^A}{d\cos\chi} = \frac{\alpha_s}{\pi}\,A(\chi) \qquad (4)$$

with $A(\chi) = F(\pi-\chi) - F(\chi)$.

Second order corrections have been recently calculated by two groups independently [3,4]. Their results can be summarized with the help of yet another function as follows

$$\frac{d\,\Sigma}{d\cos y} = \frac{\alpha_s}{\pi}\,F(\chi) + \left(\frac{\alpha_s}{\pi}\right)^2 G(\chi) = \frac{\alpha_s}{\pi}\,F(\chi)\left\{1 + \frac{\alpha_s}{\pi}\,R(\chi)\right\} \qquad (5)$$

$$\frac{d\,\Sigma^A}{d\cos\chi} = \frac{\alpha_s}{\pi}\,A(\chi) + \left(\frac{\alpha_s}{\pi}\right)^2 B(\chi) = \frac{\alpha_s}{\pi}\,A(\chi)\left\{1 + \frac{\alpha_s}{\pi}\,R^A(\chi)\right\} \qquad (6)$$

The functions $R(\chi)$ and $R^A(\chi)$, the magnitude of which gives a measurement of the importance of second order corrections, are shown in fig. 1. Please note that while the correction function is of order 20-30 for a classical jet measure like thrust and of order 1 for $\sigma_{tot}(e^+e^- \to \text{hadrons})$, it is only ~ 10 for the EEC and ~ 3 for the AEEC. Thus, as far as second order corrections are concerned, the AEEC is almost as well behaved as σ_{tot}.

In order to investigate the sensitivity of the EEC to soft radiation, rather than integrating over $0 < x_i, x_j < 1$ in Eq. (1), one restricts the available phase space to $\varepsilon < x_i, x_j < 1$. In $O(\alpha_s)$ the results can be expressed as [5]

$$\frac{d\Sigma(\varepsilon)}{d\cos\chi} = \frac{\alpha_s}{\pi}\,F(\chi,\varepsilon) \qquad (7)$$

with

$$F(\chi,\varepsilon) = F(\chi) - \frac{2}{3}\,\varepsilon\frac{1}{\xi(1-\xi)} + \varepsilon^2\,\frac{3-2\xi}{6\xi(1-\xi)} + O(\varepsilon^3) \qquad (8)$$

where $\xi = (1-\cos\chi)/2$.

The term in the r.h.s. of Eq. (8) proportional to ε is symmetric under the exchange $\chi \to \pi - \chi$, i.e. $\xi \to 1-\xi$. Thus the asymmetric component reads

$$A(\chi,\varepsilon) = A(\chi) + \varepsilon^2\,\frac{2\xi-1}{3\xi(1-\xi)} + O(\varepsilon^3) \qquad (9)$$

Power corrections of a perturbative nature affecting the AEEC are quadratic and not linear on the energy resolution parameter ε. For $\varepsilon \leq 10\%$ the asymmetry is independent of ε to better than 2%. These results are not altered if $O(\alpha_s^2)$ corrections are taken into account, see figs. 2 and 3.

Hadron production in e^+e^- annihilation is understood as a two step process. Immediately after the interaction takes place a $q\bar{q}$ pair is formed. These parent quarks emit energy and color giving rise to a parton cascade which propagates until the masses involved are close to mass-shell. Then, low energetic colored partons recombine into colorless hadrons. This second step, also known as fragmentation process, is not well understood. It is expected though that fragmentation effects behave like a power law $1/\sqrt{s}$, in contrast to the logarithmic behaviour characteristic of the perturbative terms, see Eqs. (3-6). In particular, because of the different infrared stability properties exhibited by the EEC and its related asymmetry AEEC, we expect the latter to be less sensitive to fragmentation than the former.

Any discussion of fragmentation effects is bound to be model dependent. Let me start discussing the fragmentation effects affecting the EEC in the context of the two-jet fragmentation model of Field and Feynman [6]. The expectations for the EEC at $\sqrt{s}$ = 22, 34, 45, and 60 GeV are shown in fig. 4 [5]. Notice that the height of the central plateau, $60° < \chi < 120°$, falls off like $1/\sqrt{s}$. On the other hand, the asymmetry decreases with increasing c.m. energy much faster, see fig. 5. In the large angle region i.e. close to 90°, the following parametrisation [2]

$$\frac{d\,\Sigma}{d\cos\chi} = \frac{c\,\langle p_T\rangle}{\sqrt{s}\,\sin^3\chi} \qquad (10)$$

derived in the context of a parton model with fixed $\langle p_T\rangle$ and $\langle n\rangle = B + C \ln s$, describes quite well the results obtained via Monte Carlo.

Fragmentation effects induced by gluon → hadrons are more difficult to estimate. The MARK II collaboration has proposed the ansatz [7]

$$\frac{d\,\Sigma^{q\bar{q}G}}{d\cos\chi} = \frac{\alpha_s A}{\sqrt{s}} \begin{cases} \sin^{-3}\chi, & \chi<\pi/2 \\ 1+\cos\chi, & \chi>\pi/2 \end{cases} \qquad (11)$$

with A = 2.5 ± 0.5 GeV estimated from data at a single energy namely $\sqrt{s}$ = 29 GeV. Should this estimate be realistic, then because the asymmetry component of Eq. (11) is substantial and negative, the AEEC should approach perturbative results from below, in contrast to what happens with most other jet measures like <1-T>,<jet mass> or <jet opening angle>[8]. Other estimates for the power corrections induced by the fragmentation of a gluon into hadrons can be obtained with the help of fragmentation models, be it of the independent [9] or string [10] type.

II) EXPERIMENTAL DETAILS

The data presented in this analysis have been obtained by the TASSO and PLUTO collaborations, working at the e^+e^- storage ring PETRA at DESY. Hadronic events were selected using standard criteria[11,12]. The TASSO sample consists of 2697 events at 14 GeV, 1902 at 22 GeV, 20523 at 34 GeV and 4436 at 43 GeV. The PLUTO sample consists of 6964 events at 34 GeV.

In order to obtain the EEC, use has been made of charged particles only, for reasons of better angular accuracy. Corrections for initial state radiation, selection criteria, acceptance and resolution have been calculated with the help of standard Monte Carlo techniques.

III) RESULTS

a) On low order perturbation theory effects

We show in figs. 6, 7, 8 and 9 the corrected EEC data along with a comparison to the linear sum of a perturbative term given by Eq. (5) and a fragmentation component which we parametrise by Eq. (10). Using this ansatz involving only two free parameters, a good description of the energy and angular dependence exhibited by the data is obtained, provided we stay away from the regions

near χ = 0, π, i.e. $|\cos\chi| < 0.8$.

The central plateau in the EEC is falling off sharply with increasing energy. This is perhaps more clearly illustrated in fig. 10 where we present EEC data integrated in the region $|\cos\chi| < 0.5$ as a function of energy. Data from the PLUTO collaboration has also been included[12]. The solid line represents the results of a fit to the ansatz discussed previously. Best estimates for the two parameters involved are $\Lambda_{\overline{MS}}$ = 350 ± 66 MeV and C $\langle p_T \rangle$ = 0.85 ± 0.16 GeV.

We are aware of the fact that the approach adopted is naive and limited in scope. It serves however to illustrate that, in order to describe the large angle behaviour of the EEC data, in addition to the perturbative results only a term characteristic of the two jet fragmentation contribution is needed.

If our picture is consistent the AEEC at large angles should exhibit a very slight energy dependence. That this is indeed so, is shown in fig. 11. We plot the AEEC data in a way reminiscent of what we do when looking for scaling violations in inclusive spectra, i.e. we show the data as a function of $\sqrt{s}$ for various cos χ bins. Notice that strong scaling violations are observed for values cos $\chi \sim 1$, the region where the fragmentation of two-jet events is very important. As cos χ becomes smaller the scaling violation effects become much less important. In fact the energy dependence of the AEEC integrated in the region $|\cos\chi| < 0.80$, see fig. 12, is consistent with the logarithmic behaviour predicted in perturbation theory, Eq. (6). A fit to the data yields for the single free parameter involved $\Lambda_{\overline{MS}}$ = 100 ± 20 MeV, corresponding to $\alpha_s(\sqrt{s}$ = 43 GeV) = 0.12. Indeed, not only the energy, but also the large angle dependence of the AEEC is described by the bare QCD prediction, Eq (6), with the value of $\Lambda_{\overline{MS}}$ given above. This is illustrated in fig. 13. The fact that the bare QCD prediction does not describe the data at cos χ values near 1 is expected since the small angle region is dominated by fragmentation effects. Even the perturbative calculation, as we will discuss later should not be trusted at such angles where multigluon effects must be taken into account.

Of course if we want to describe the AEEC data in the entire

angular region we are forced to consider fragmentation models. We consider both the independent fragmentation scheme by Ali et al.[9] and the string model as developed by the LUND group[10]. Second order corrections are included as discussed in ref. 6) using (ε,δ) cut-offs to separate two from three and four-jet events. The values obtained for α_s at $\sqrt{s}$ = 43 GeV are 0.136 ± 0.010 (Ali et al.) and 0.140 ± 0.010 (Lund). They are to be compared to those previously published by the TASSO collaboration at 34 GeV, namely 0.127 ± 0.010 (Ali et al.) and 0.159 ± 0.012 (Lund). Both fragmentation schemes give the same description of the data, see full-lines in figs. 14 a,b,c. To further illustrate that the large angle AEEC is a genuine hard gluon bremsstrahlung effect we also show in fig. 14 the expectations obtained in the Field-Feynman model, dashed-dotted line, as well as in the original version of the Webber Monte Carlo[13] based on a QCD calculation taking into account multiple soft gluon emission in the leading log approximation.

In order to illustrate the systematic uncertainties involved in the determination of $\Lambda_{\overline{MS}}$ we show in fig. 15 the values obtained by the PLUTO collaboration using the different approaches discussed in the text.

b) On effects due to perturbation theory at all orders

It was already emphasized in the early work of KUV[14] and DDT[15] that the EEC also offers, in principle, the possibility of testing higher order QCD effects, by looking at angles $0 \ll \chi \ll 90$ where calculations in the leading logarithmic approximation were performed[14] and near the back-to-back configuration where results based on the double logarithmic approximation can be found[15].

The experimental work done in this field by the PLUTO collaboration[16] has shown that at energies presently available fragmentation effects are important in the small angular regions were LLA calculations are supposed to be valid. This together with the uncertainties intrinsic in the calculations themselves, made quantitative comparisons between data and theory not conclusive.

Recent calculations by Collins and Soper, who make use of renormarlization group techniques to obtain results at all orders in perturbation theory, have arosen renewed interest on the EEC in

the back-to-back configuration[17]. These authors also provide an estimate of the fragmentation effects induced by two-jet events using parton model arguments similar in content to those discussed when referring to Eq. (10).

This together with the fact that in the last year PETRA has accumulated some luminosity at an energy, $\sqrt{s}$ = 43 GeV, higher than that available in previous analysis[16] prompted us to make a comparison between our data and Collins and Soper prediction. This is illustrated in figs. 16-17-18-19. Fits were performed to the data in the angular region $0 < 1 - \cos\theta < 0.05$, θ being the acollinearity angle i.e. $\theta = \pi - \chi$, and the results extrapolated to the whole backward hemisphere. The results are very encouraging, although it is not completeley satisfactory to see that fragmentation effects are still large, since they are parametrised with an ad-hoc function.

IV) CONCLUSIONS

The AEEC is a measure characterising the hadronic final states produced in e^+e^- annihilation, which satisfies very convenient properties, like being insensitive to higher order corrections in perturbation theory as well as being infrared stable. Because of this, one expects the AEEC to behave very smoothly with center of mass energy.

The data in the range $14 \leq \sqrt{s} \leq 43$ GeV show indeed a very mild energy dependence, similar to that exhibited by $R = \sigma(e^+e^- \to \text{hadrons})/\sigma(e^+e^- \to \mu^+\mu^-)$. Not only the energy dependence but also the large angle behaviour of the AEEC is in agreement with perturbative QCD predictions in $O(\alpha_s^2)$. The AEEC at small angles is however dominated by effects due to the fragmentation of two-jet events. Thus, in order to describe the AEEC in the complete angular range, one has to resort to comparisons with Monte Carlo fragmentation models. Values for α_s obtained at $\sqrt{s}$ = 43 GeV using various approaches lie between 0.120 and 0.145. These numbers are in fair agreement with those obtained by other collaborations[1,3,12,18,19] provided second order corrections are included following Ref. 3).

The EEC data in the back-to-back configuration is very nicely described by perturbative results at all orders supplemented with an ad-hoc parametrisation of fragmentation effects. The latter are at present energies non-negligible.

ACKNOWLEDGEMENTS

I would like to thank my colleagues in the PLUTO and TASSO collaborations, G. Kreutz and L. Labarga in particular, for help in preparing this note. I am grateful to Prof. Brandt in Siegen and Prof. C. López in Madrid, for their support. Discussions with A. Ali, E. Lohrmann and D. Soper are gratefully acknowledged. I thank J. Grunhaus and P. Söding for their efforts to organize a superb Meeting in Kyriat-Anavim. Last but not least I would like to thank Frau U. Bender for typing the manuscript.

REFERENCES

1) F. Barreiro, Habilitationsschrift, Siegen University, Fortschritte der Physik, to appear.
2) L.S. Brown, C.L. Bashan, S.D. Ellis and S.T. Love, Phys. Rev. Lett. 41 (1978) 1525.
3) A. Ali and F. Barreiro, Phys. Lett. 118B (1982) 155.
4) D. Richards, W. Stirling, And S.D. Ellis, Phys. Lett. 119B (1982) 193.
5) A. Ali and F. Barreiro, Nucl. Phys. B236 (1984) 269.
6) R.D. Field and R.P. Feynman, Nucl. Phys. B136 (1978) 1.
7) MARK II Collaboration, D. Schlatter et al., Phys. Rev. Lett 49 (1982) 251.
8) PLUTO Collaboration, Ch. Berger et al., Z. Phys. C12 (1982) 297.
9) A. Ali, private communication.
10) T. Sjöstrand, Comp. Phys. Comm. 27 (1982) 24B and 28 (1983) 229.
11) TASSO Collaboration, M Althoff et al., Phys. Lett. 138B (1984) 441.
12) F. Barreiro, in the Proceedings of the XIX Rencontres de Moriond, Trahn Than Vahn Editor, 1984
PLUTO Collaboration, Ch. Berger et al., DESY 85-039.
13) B. Webber, Nucl. Phys. B238 (1984) 492.
14) K. Konishi, A. Ukawa and G. Veneziano, Phys. Lett. 80B, (1978) 259.

15) Y. Dokshitzer, D. Dyakonov and S. Troyan, Phys. Lett. 78B (1981) 290.
16) PLUTO Collaboration, Ch. Berger et al., Phys. Lett. 99B (1981) 292.
17) J. Collins and D.E. Soper, University of Oregon preprint, OITS 273, March 1985.
18) MARK J Collaboration, B. Adeva et al., Phys. Rev. Lett. 50 (1983) 2051, and MIT-LNS-142, 1985.
19) TASSO Collaboration, M.Althoff et al., Z. Phys. C26 (1984) 157.

FIGURE CAPTIONS

Fig. 1: Second order correction functions for the EEC and its related asymmetry. Solid line represents a fit to the Monte Carlo points obtained in ref. 5.
Fig. 2: The dependence of the F and G functions, see text for definitions, on the energy resolution parameter.
Fig. 3a: The dependence of the A and B functions, see text for definitions, on the energy resolution parameter.
Fig. 3b: The dependence of the $O(\alpha_s^2)$ asymmetry on the energy resolution parameter
Fig. 4: The expectations from the Field-Feynman model for the two-jet contribution to the EEC.
Fig. 5: The expectations from the Field-Feynman model for the two-jet contribution to the AEEC.
Fig. 6: The EEC data at 14 GeV. Solid line represents the result of a fit to the linear sum of the $O(\alpha_s^2)$ prediction and a fragmentation term, see text for details.
Fig. 7,8,9: Same as fig. 6 at 22, 34 and 43 GeV, respectively.
Fig. 10: The EEC data integrated for $|\cos\chi| < 0.5$ as a function of $\sqrt{s}$.
Fig. 11: The TASSO data on AEEC as a function of c.m. energy for various χ bins.
Fig. 12: The AEEC data integrated for $|\cos\chi| < 0.8$ as a function of $\sqrt{s}$.
Fig. 13a: The AEEC, (14, 34, 43 GeV), measured by the TASSO Collaboration along with a comparison to the bare second order QCD prediction, with $\Lambda_{\overline{MS}} = 100$ MeV.
Fig. 13b: Same for the PLUTO data.

Fig. 14a,b: TASSO data for the AEEC at 34 and 43 GeV, respectively. Dashed-dotted line represents the expectations for the two-jet contribution according to Field-Feynman. The dashed line represents the expectations from Webber Monte Carlo based on a parton shower. The solid line represents the expectations from Monte Carlo including three and four-jet events, fragmenting independently or via "strings".

Fig. 14c: Same for PLUTO data at 34 GeV.

Fig. 15: Values for $\Lambda_{\overline{MS}}$ obtained by the PLUTO Collaboration.

Fig. 16-17-18-19: The EEC data in the backward hemisphere at 14, 22, 34 and 43 GeV, respectively. Solid curves represent the results of a fit to Collins-Soper predictions.

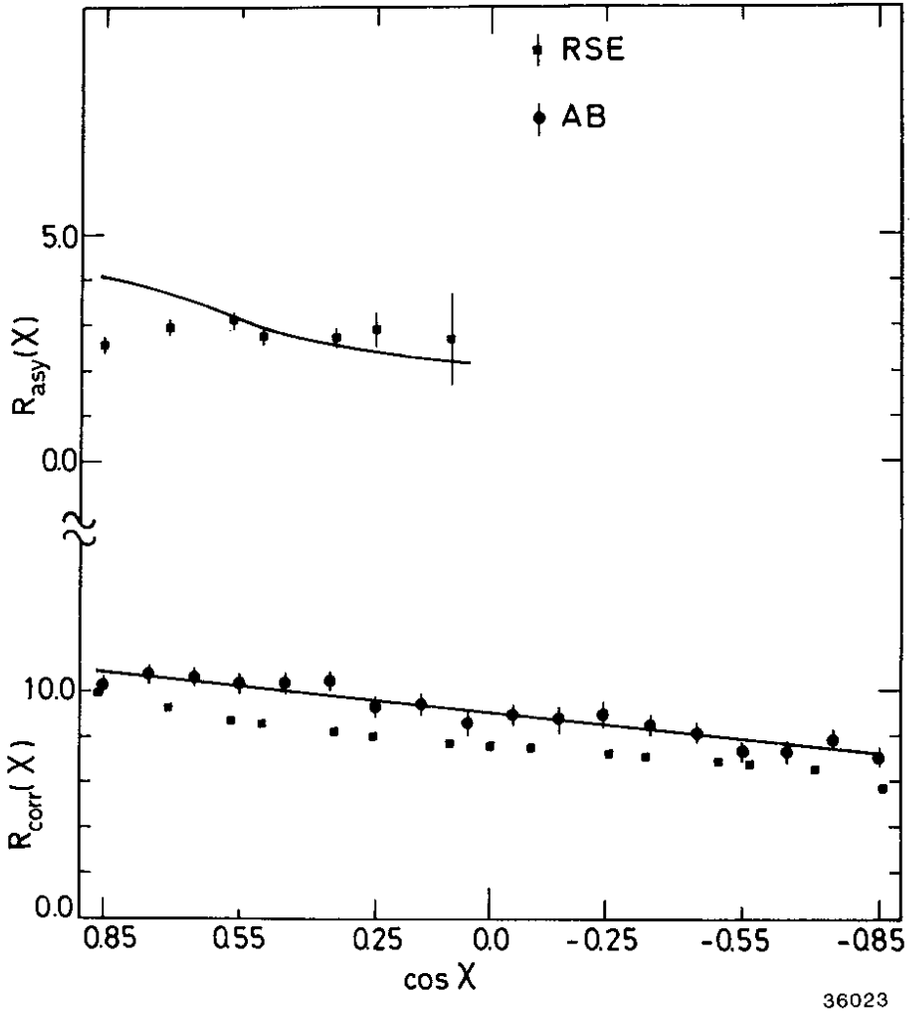

Fig. 1

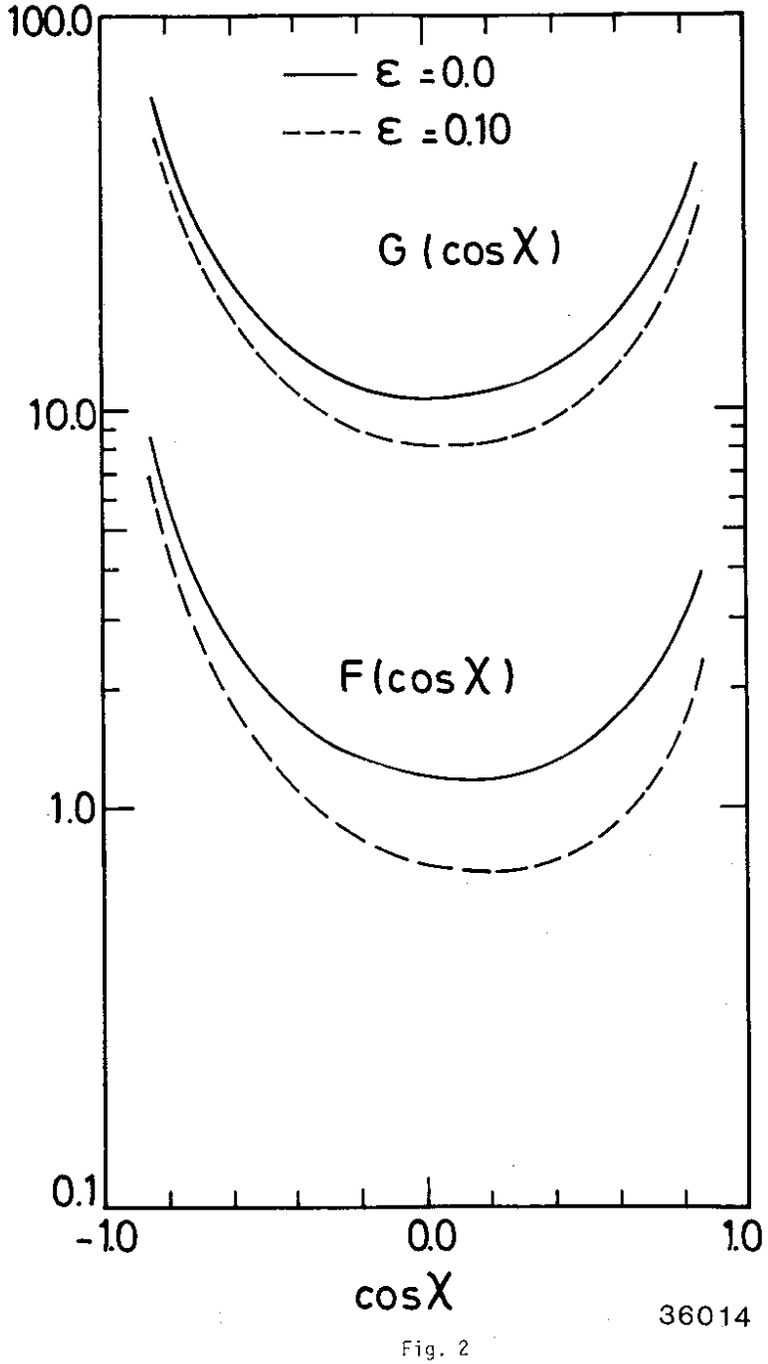
100.0
10.0
1.0
0.1
ε =0.0
ε =0.10
G (cos X)
F(cos X)
-1.0
0.0
1.0
cos X
36014

Fig. 2

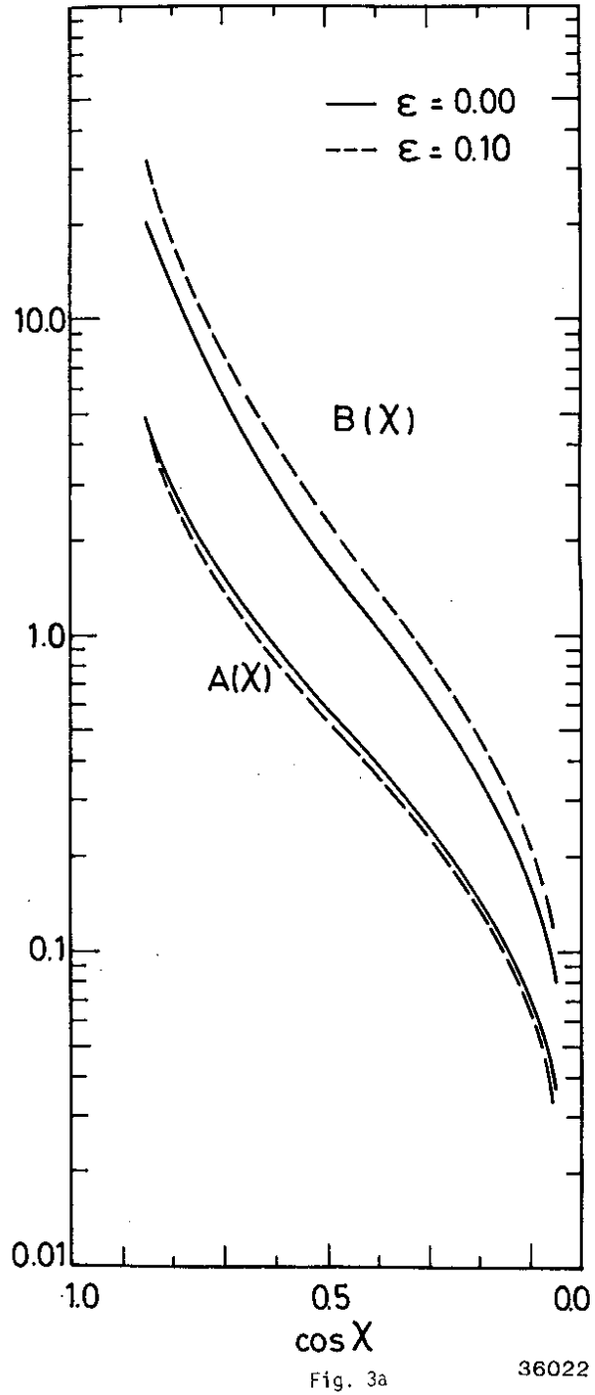
ε = 0.00
ε = 0.10
B(X)
A(X)
10.0
1.0
0.1
0.01
1.0
0.5
0.0
cos X
36022

Fig. 3a

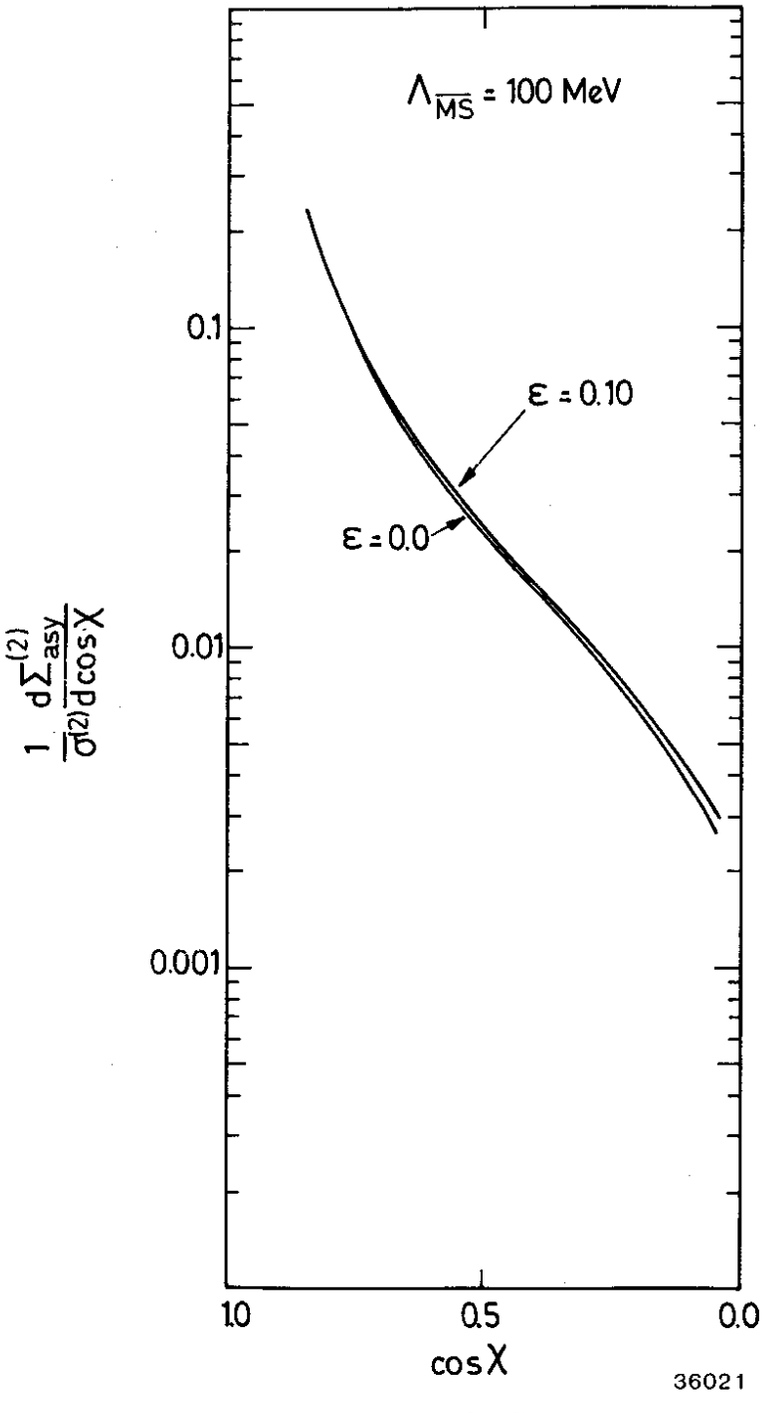
$\Lambda_{\overline{MS}}$ = 100 MeV
ε = 0.10
ε = 0.0
0.1
0.01
0.001
1.0
0.5
0.0
cosχ
$\frac{1}{\sigma^{(2)}} \frac{d\Sigma^{(2)}_{asy}}{d\cos\chi}$
36021

Fig. 3b

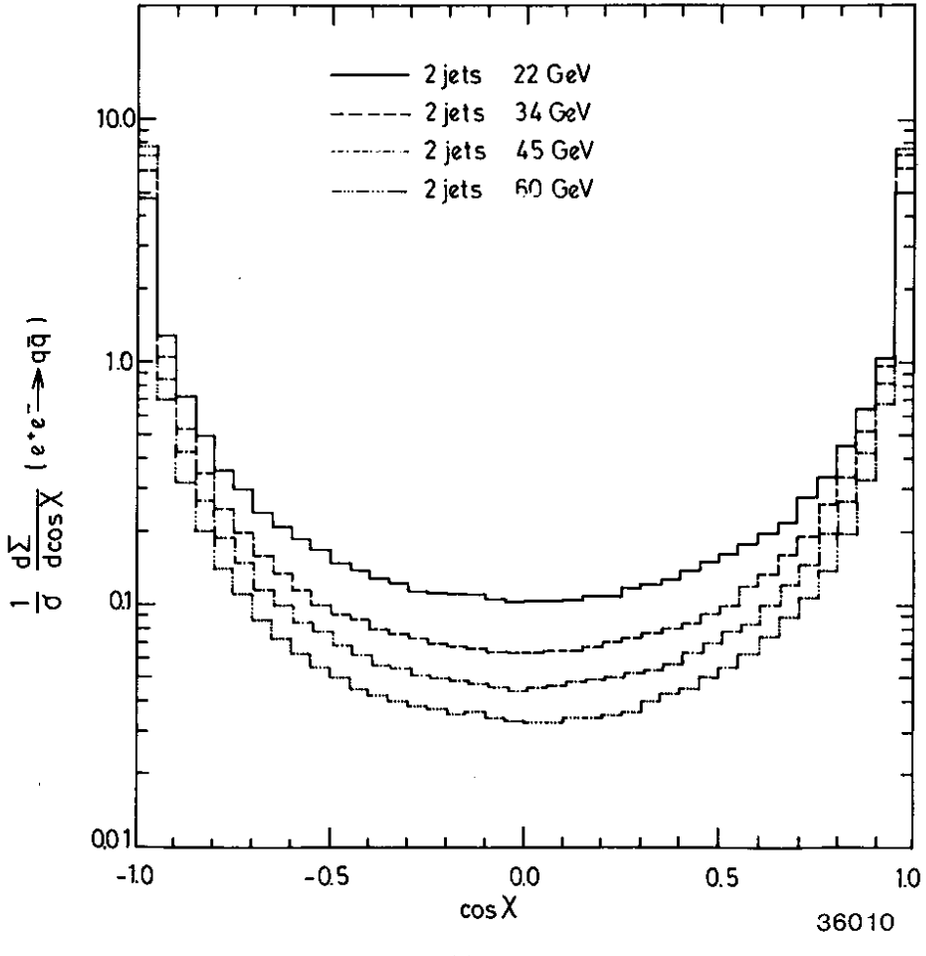
2 jets 22 GeV
2 jets 34 GeV
2 jets 45 GeV
2 jets 60 GeV
10.0
1.0
0.1
0.01
-1.0
-0.5
0.0
0.5
1.0
cosχ
$\frac{1}{\sigma} \frac{d\Sigma}{d\cos\chi}$ ($e^+e^- \to q\bar{q}$)
36010

Fig. 4

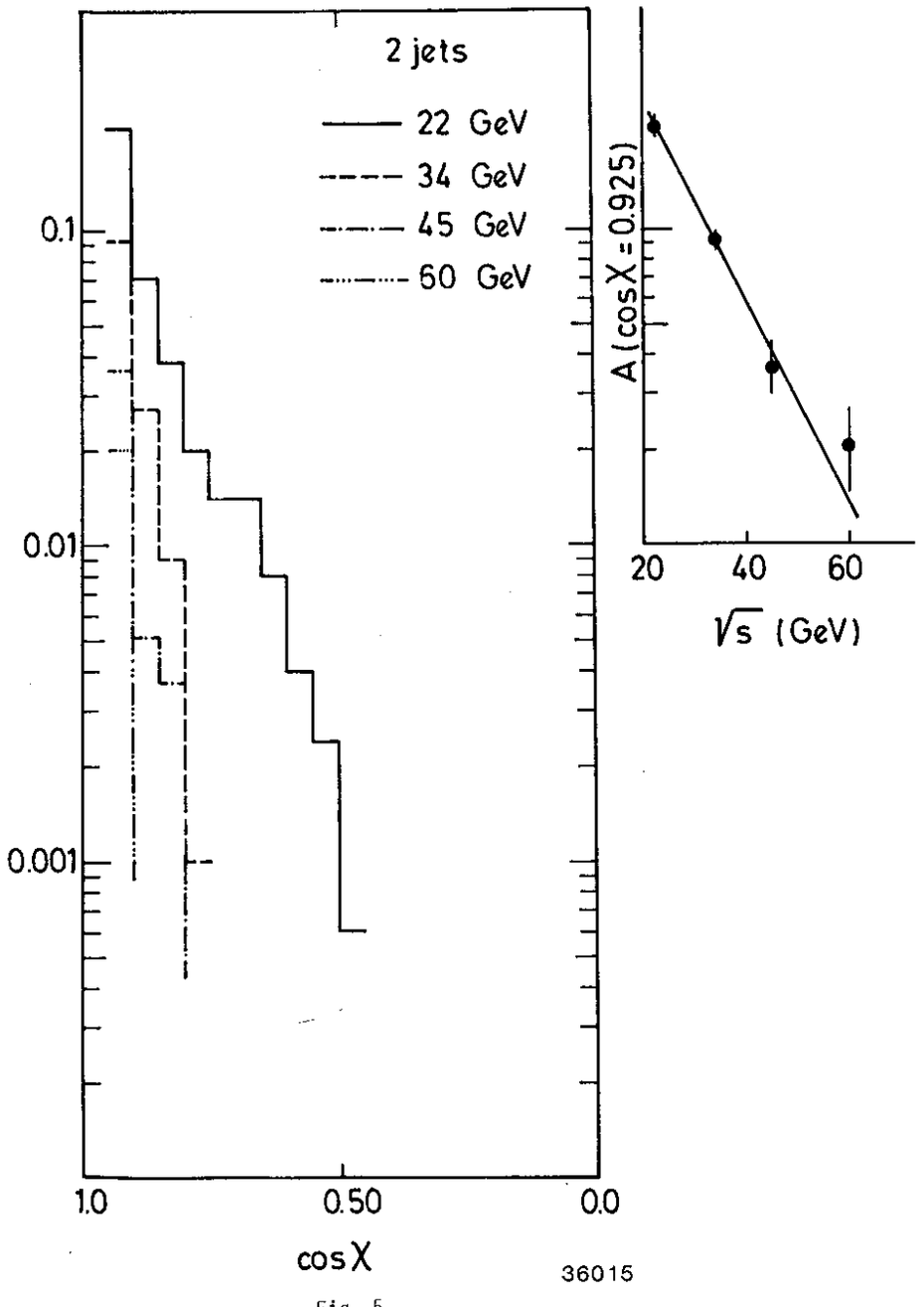
2 jets
22 GeV
34 GeV
45 GeV
60 GeV
0.1
0.01
0.001
1.0
0.50
0.0
cos X
A(cos X = 0.925)
20
40
60
√s (GeV)
36015

Fig. 5

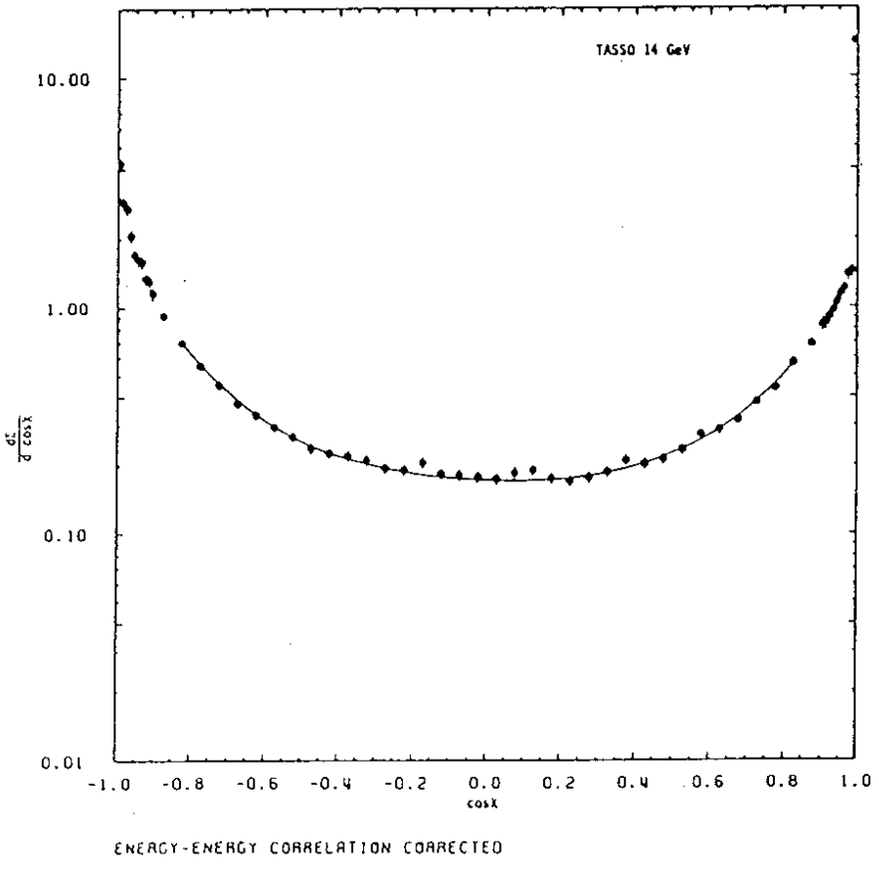
TASSO 14 GeV
10.00
1.00
0.10
0.01
-1.0
-0.8
-0.6
-0.4
-0.2
0.0
0.2
0.4
0.6
0.8
1.0
cosχ
ENERGY-ENERGY CORRELATION CORRECTED

Fig. 6

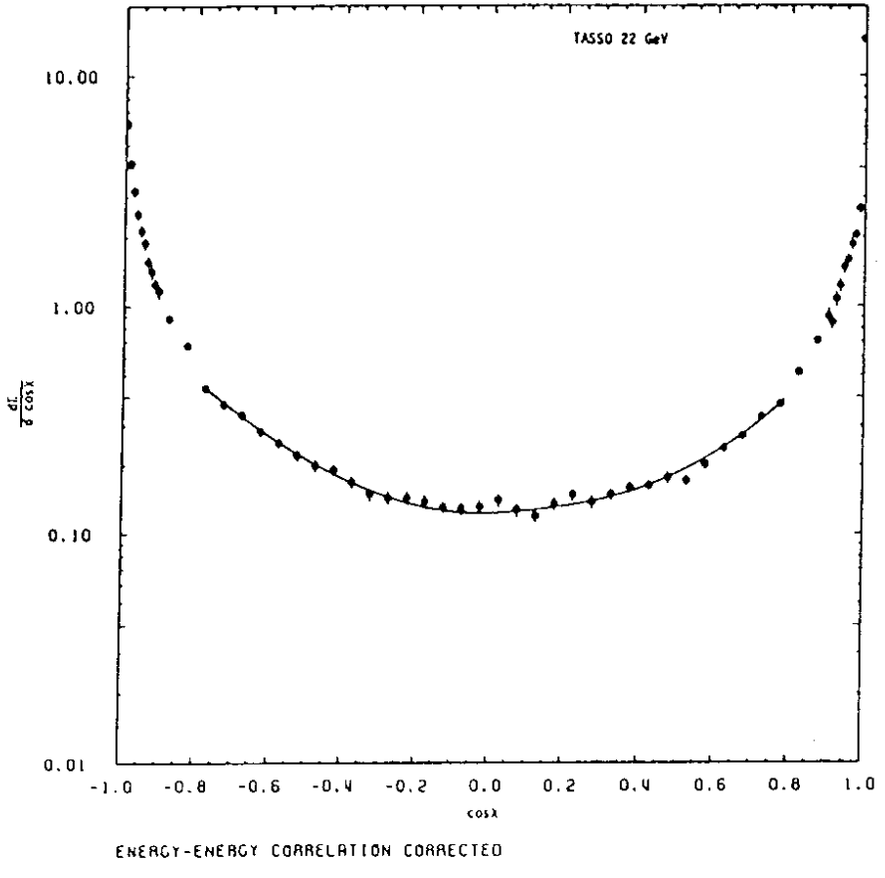
TASSO 22 GeV
10.00
1.00
0.10
0.01
-1.0
-0.8
-0.6
-0.4
-0.2
0.0
0.2
0.4
0.6
0.8
1.0
cosχ
ENERGY-ENERGY CORRELATION CORRECTED

Fig. 7

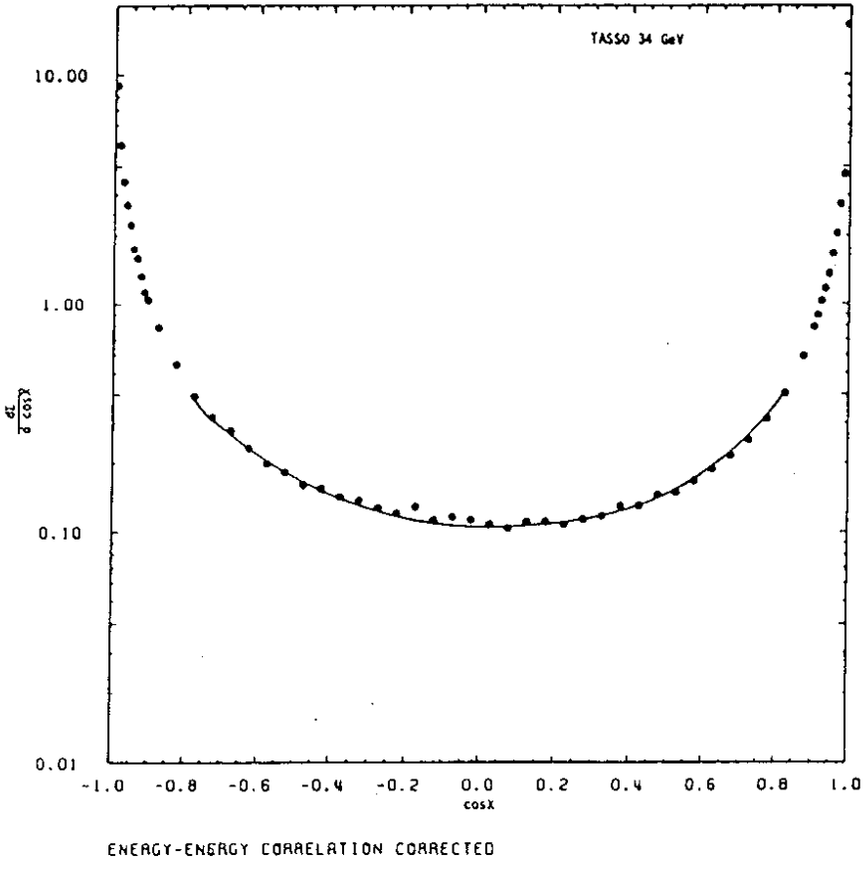
TASSO 34 GeV
10.00
1.00
0.10
0.01
-1.0
-0.8
-0.6
-0.4
-0.2
0.0
0.2
0.4
0.6
0.8
1.0
cosχ
ENERGY-ENERGY CORRELATION CORRECTED

Fig. 8

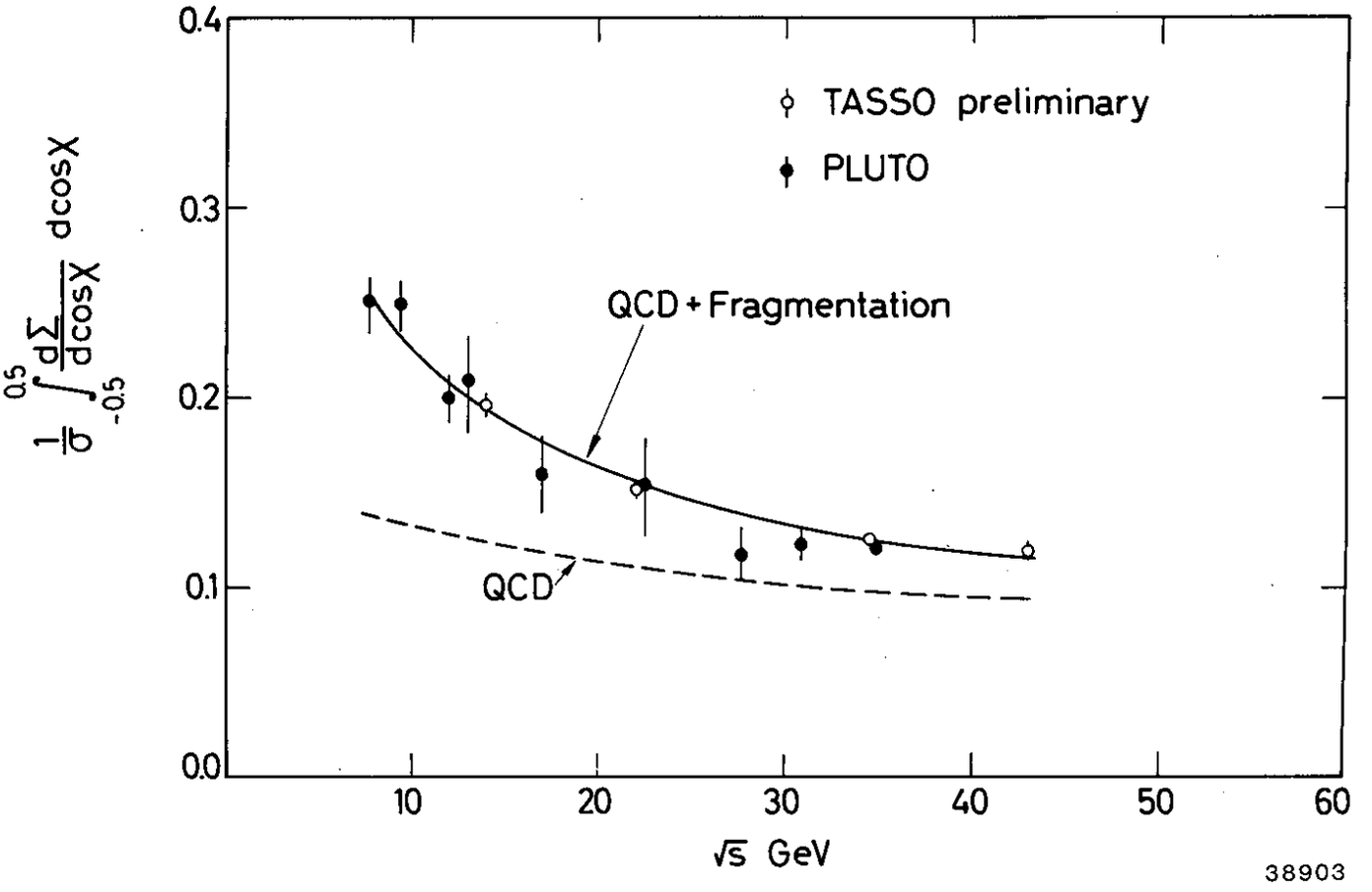
$\frac{1}{\sigma}\int_{-0.5}^{0.5}\frac{d\Sigma}{d\cos\chi}\,d\cos\chi$
TASSO preliminary
PLUTO
QCD + Fragmentation
QCD
0.4
0.3
0.2
0.1
0.0
10
20
30
40
50
60
$\sqrt{s}$ GeV
38903

Fig. 1o

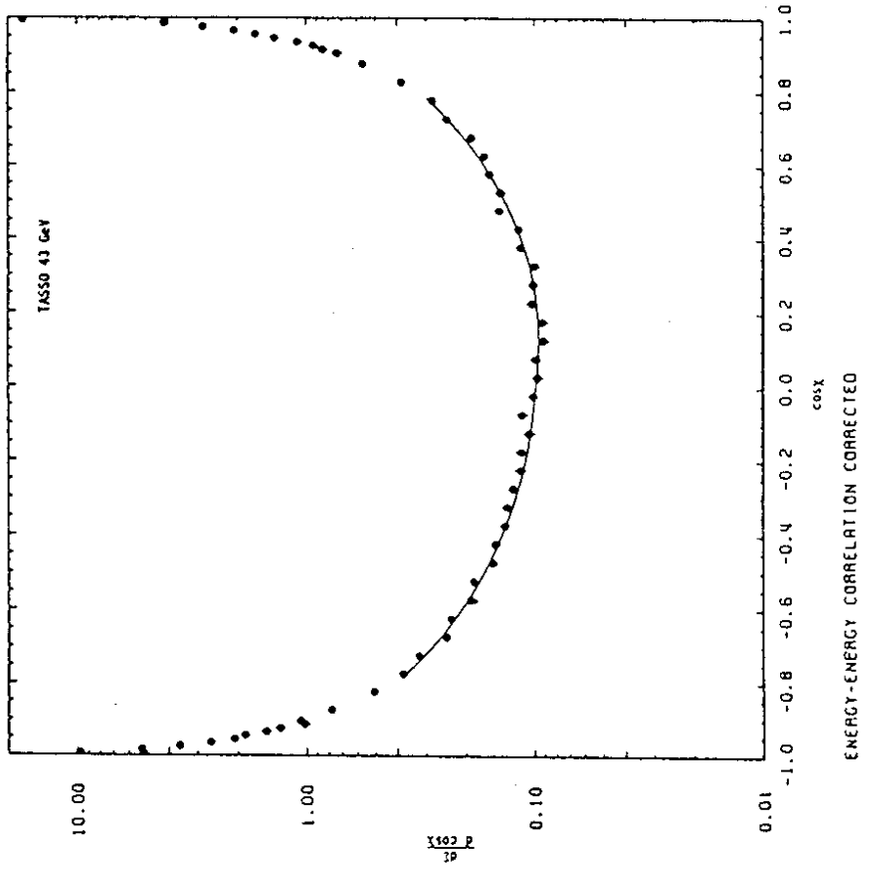
TASSO 43 GeV
10.00
1.00
0.10
0.01
1.0
0.8
0.6
0.4
0.2
0.0
-0.2
-0.4
-0.6
-0.8
-1.0
cosχ
ENERGY-ENERGY CORRELATION CORRECTED

Fig. 9

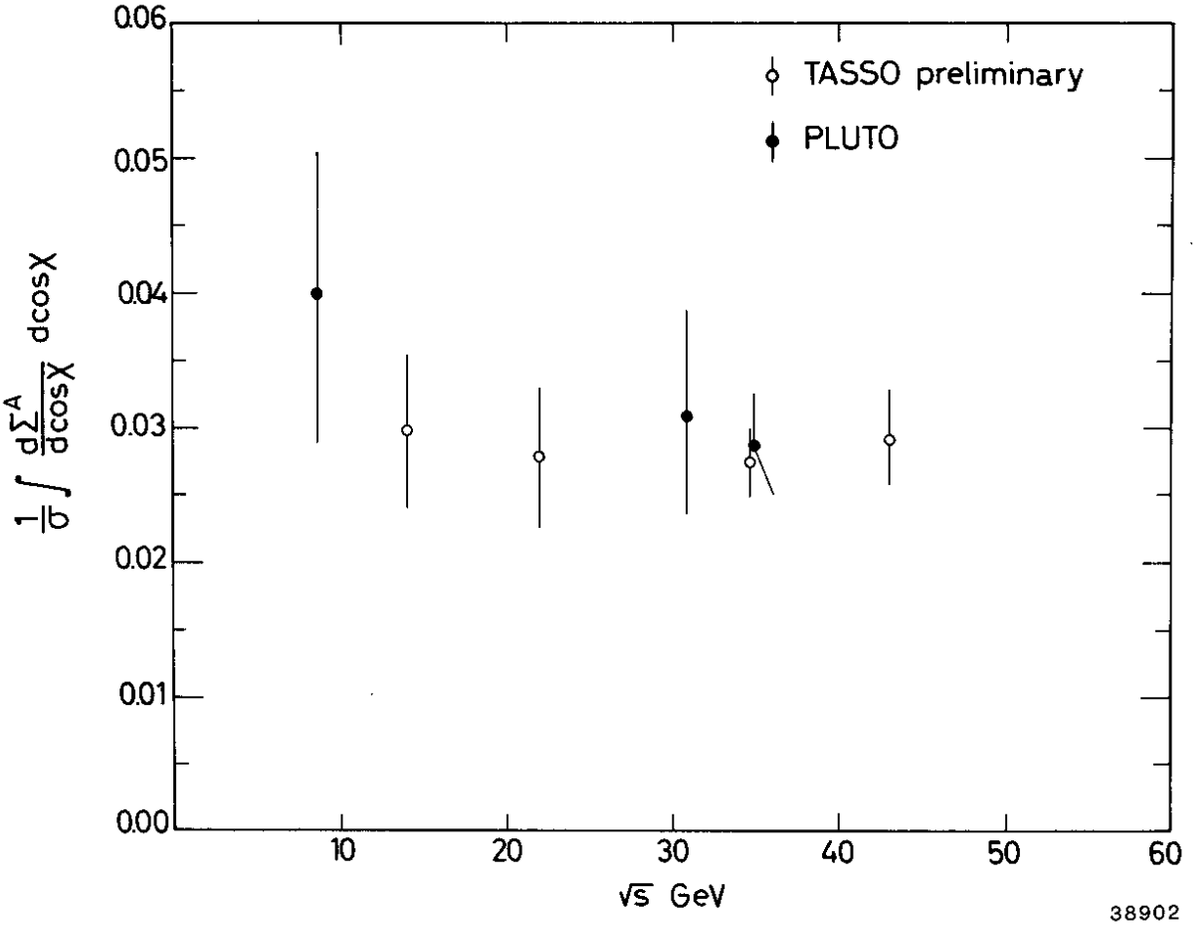
TASSO preliminary
PLUTO
$\frac{1}{\sigma}\int \frac{d\Sigma^A}{d\cos\chi} d\cos\chi$
$\sqrt{s}$ GeV
38902

Fig. 12

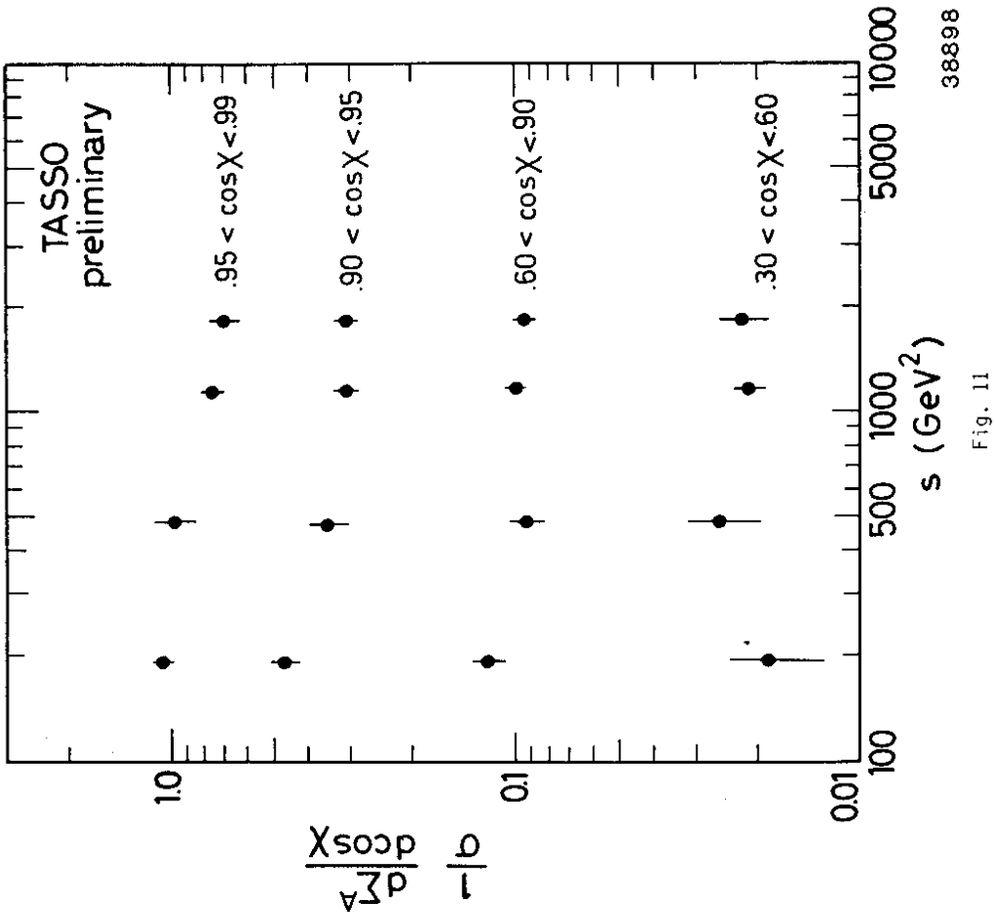
TASSO
preliminary
.95 < cosχ <.99
.90 < cosχ <.95
.60 < cosχ <.90
.30 < cosχ <.60
$\frac{1}{\sigma}\frac{d\Sigma^A}{d\cos\chi}$
s (GeV^2)
38898

Fig. 11

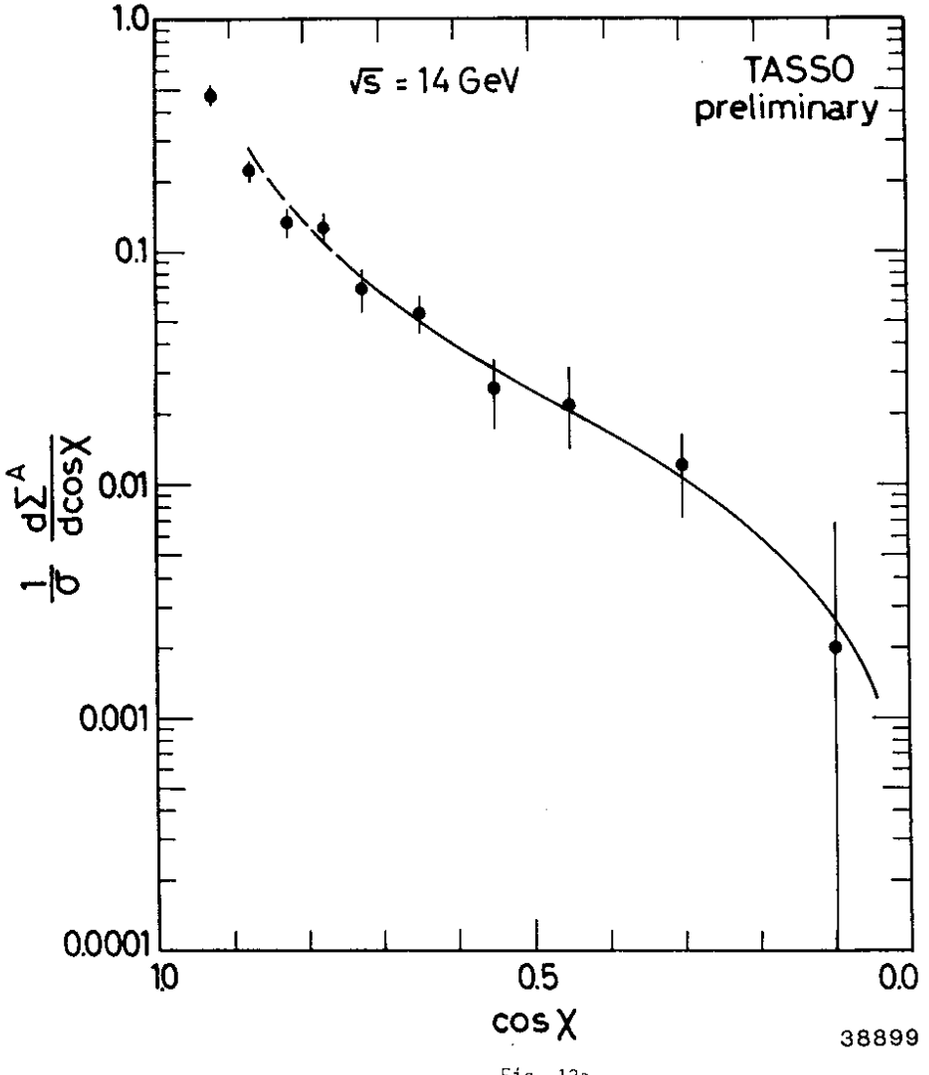

Fig. 13a

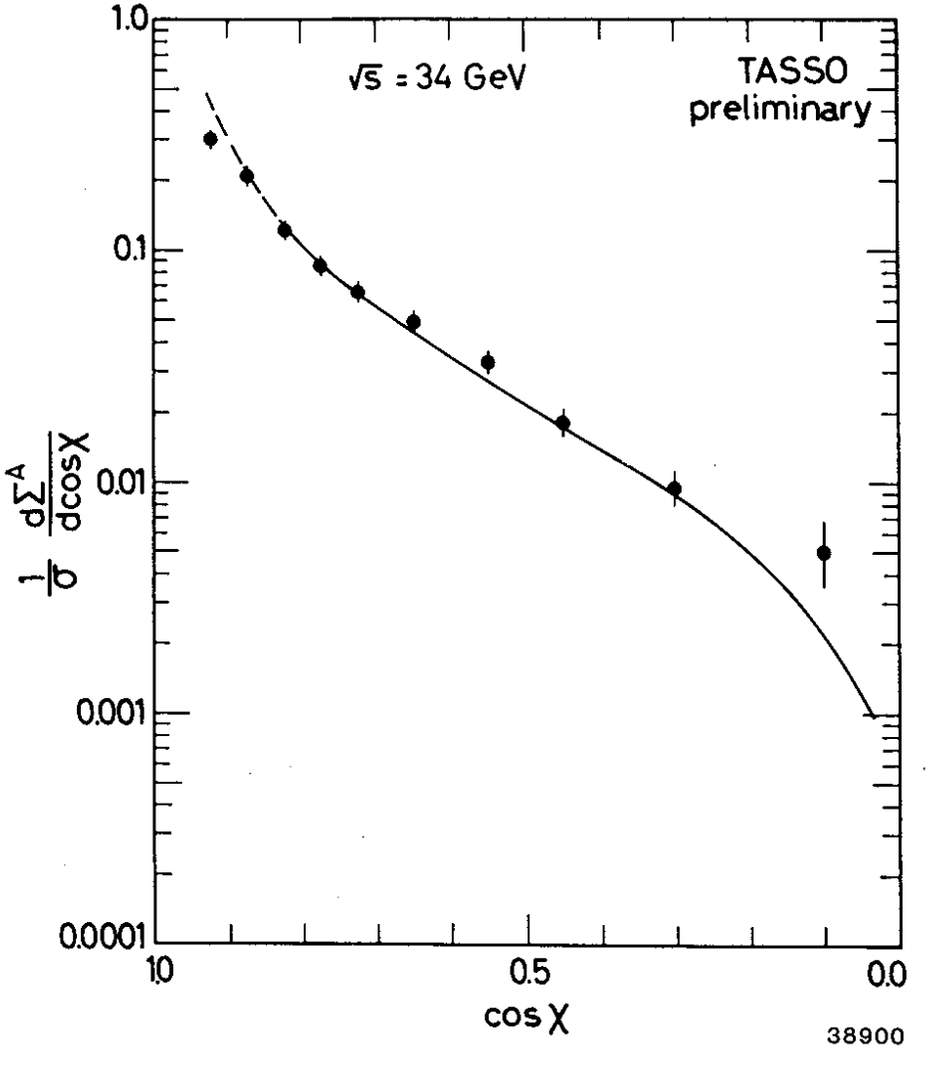

Fig. 13a

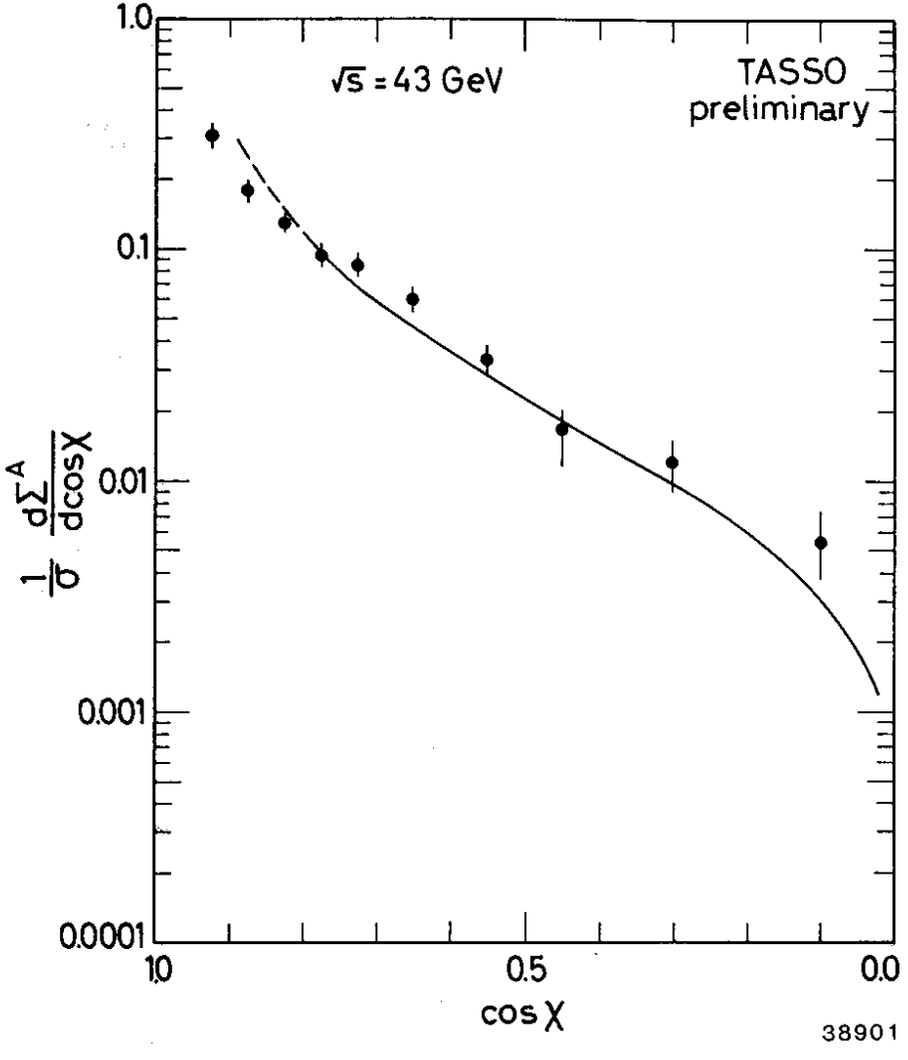

Fig. 13a

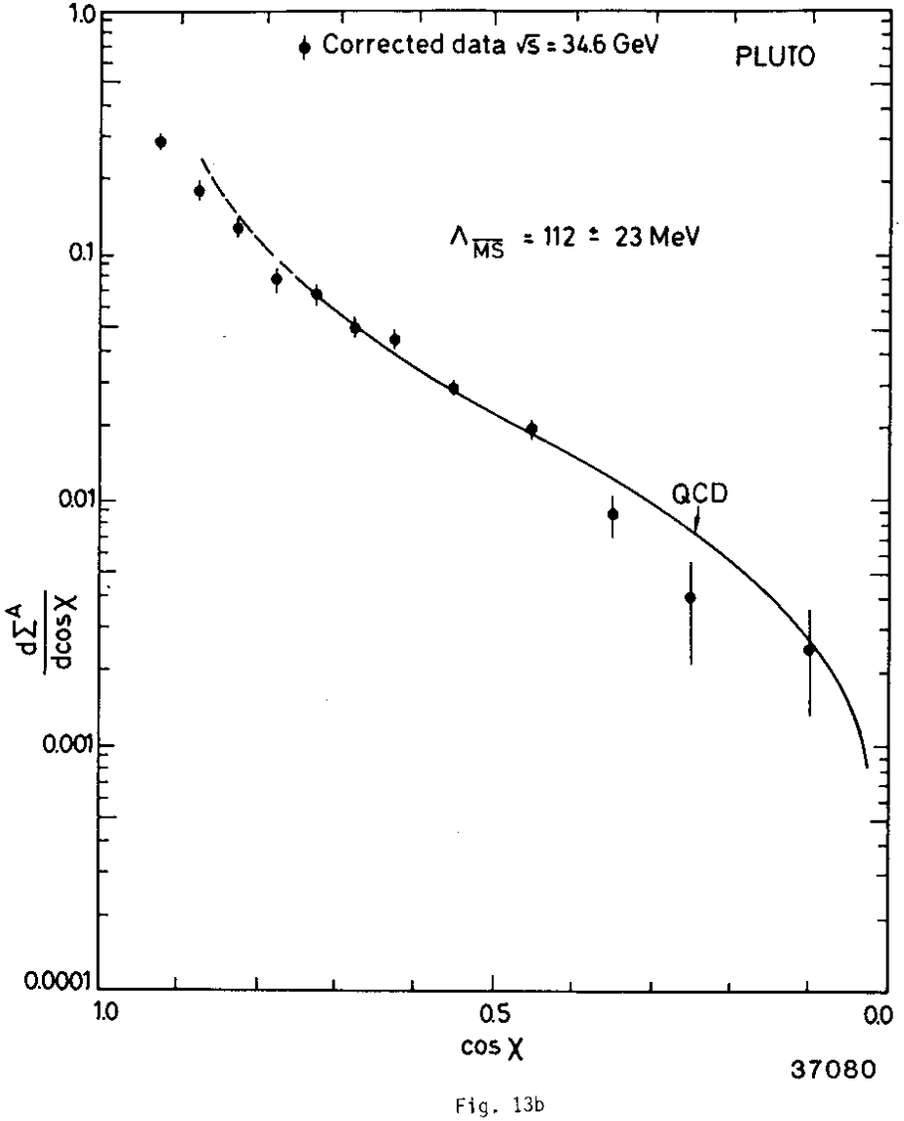

Fig. 13b

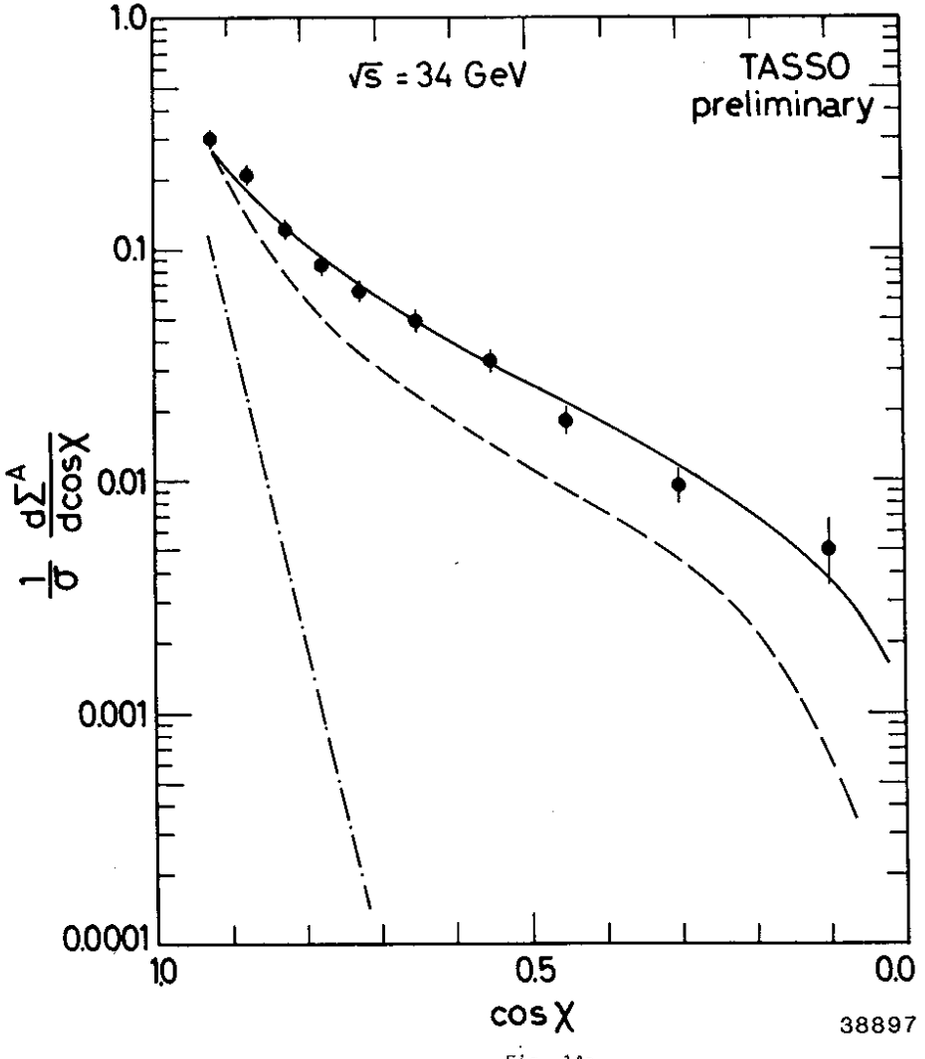

Fig. 14a

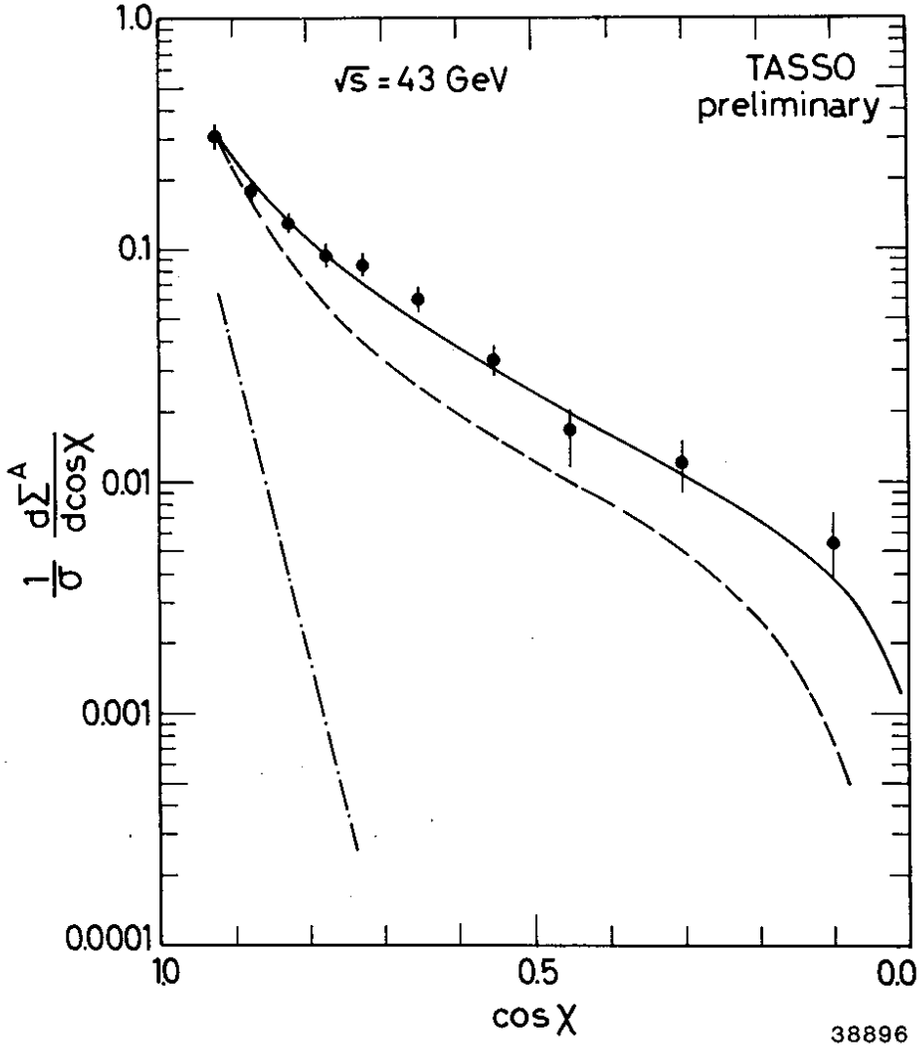

Fig. 14b

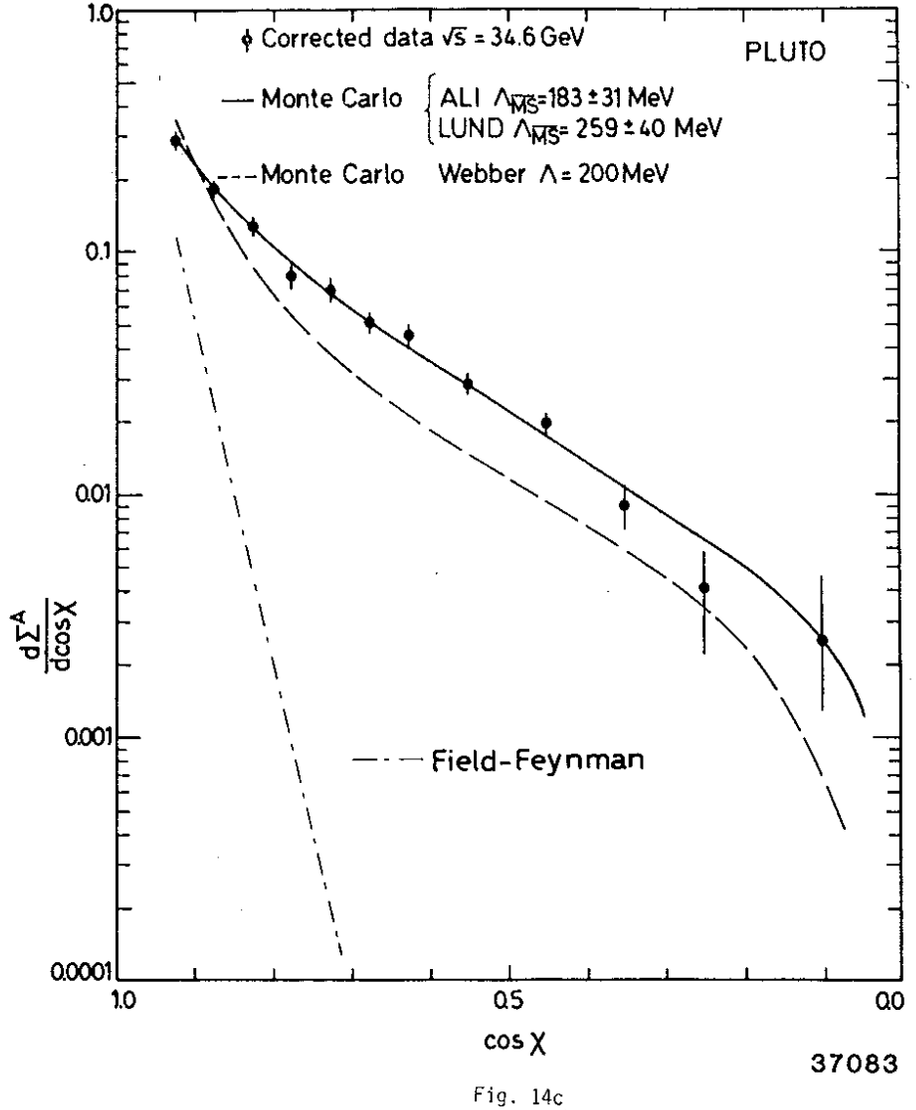

Fig. 14c

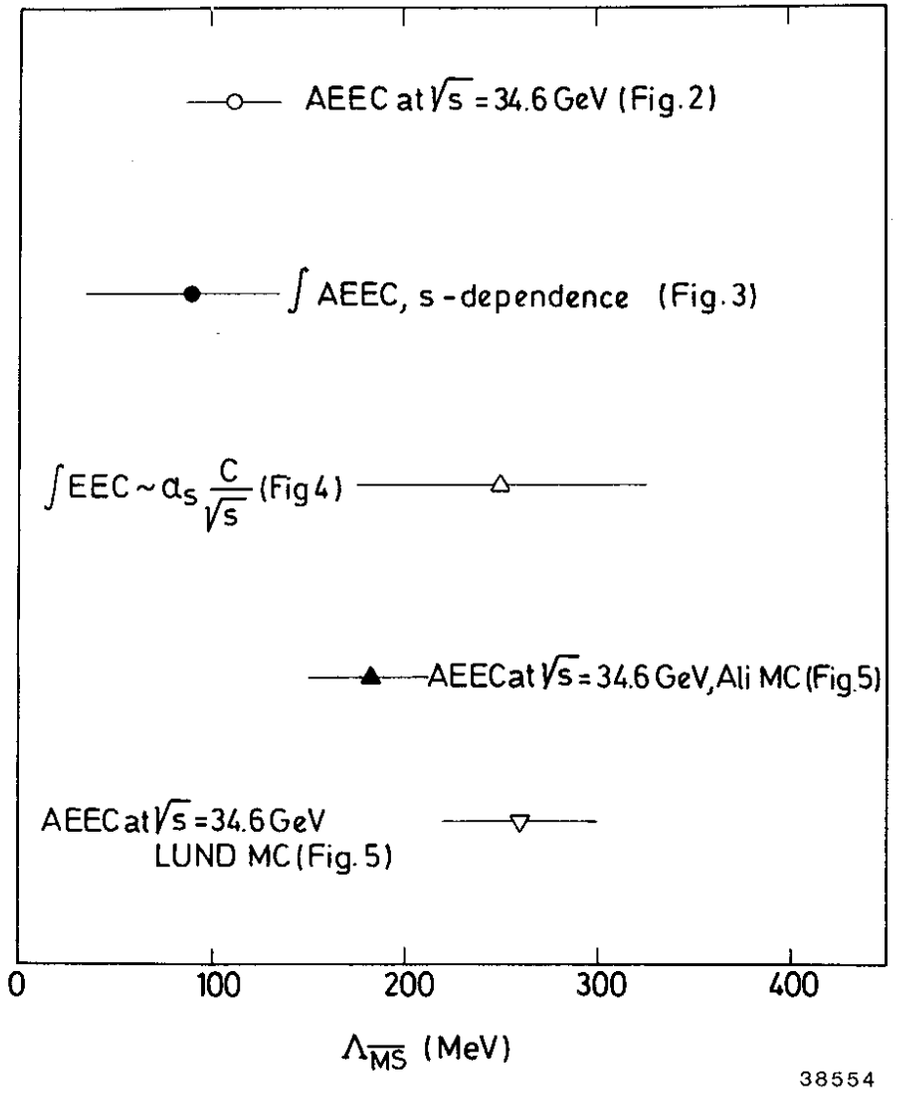

Fig. 15

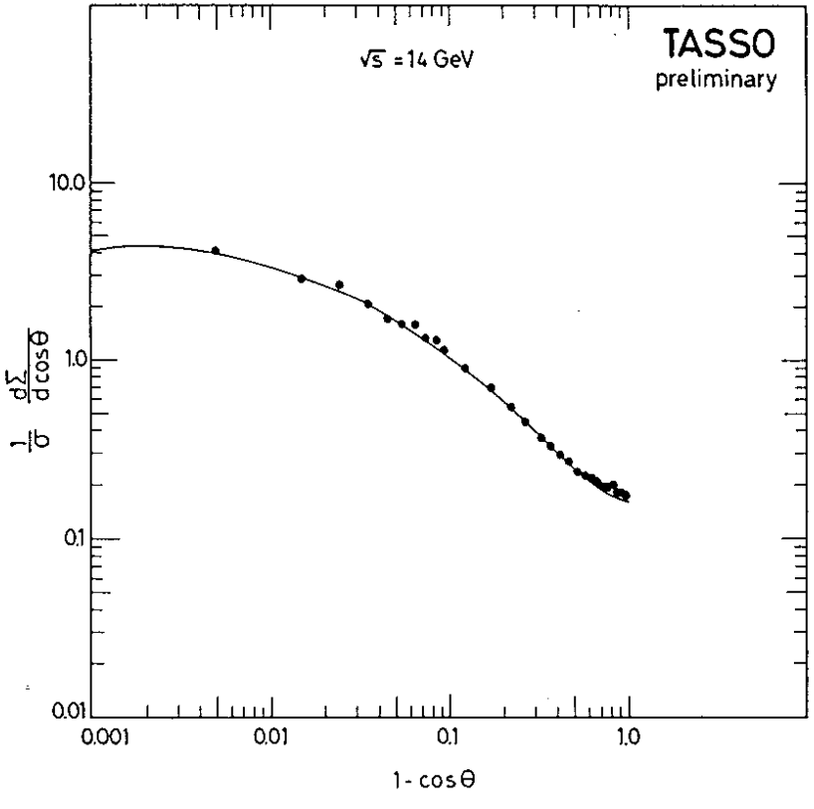
TASSO
preliminary
√s = 14 GeV
10.0
1.0
0.1
0.01
0.001
0.01
0.1
1.0
1- cosΘ
1/σ dΣ/d cosΘ

Fig. 16

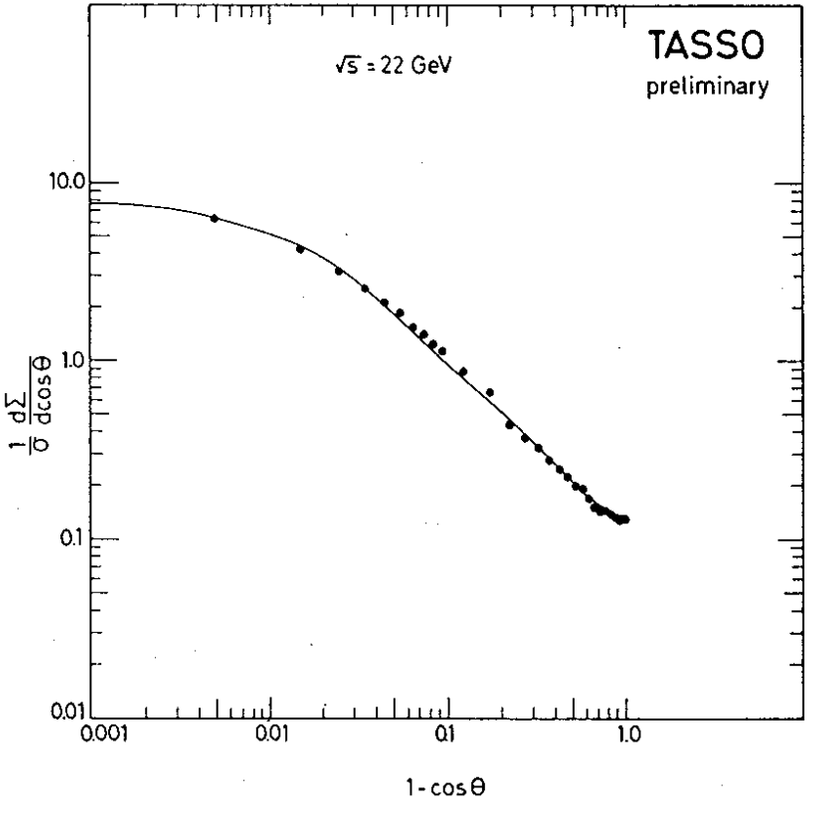
TASSO
preliminary
√s = 22 GeV
10.0
1.0
0.1
0.01
0.001
0.01
0.1
1.0
1- cosΘ
1/σ dΣ/d cosΘ

Fig. 17

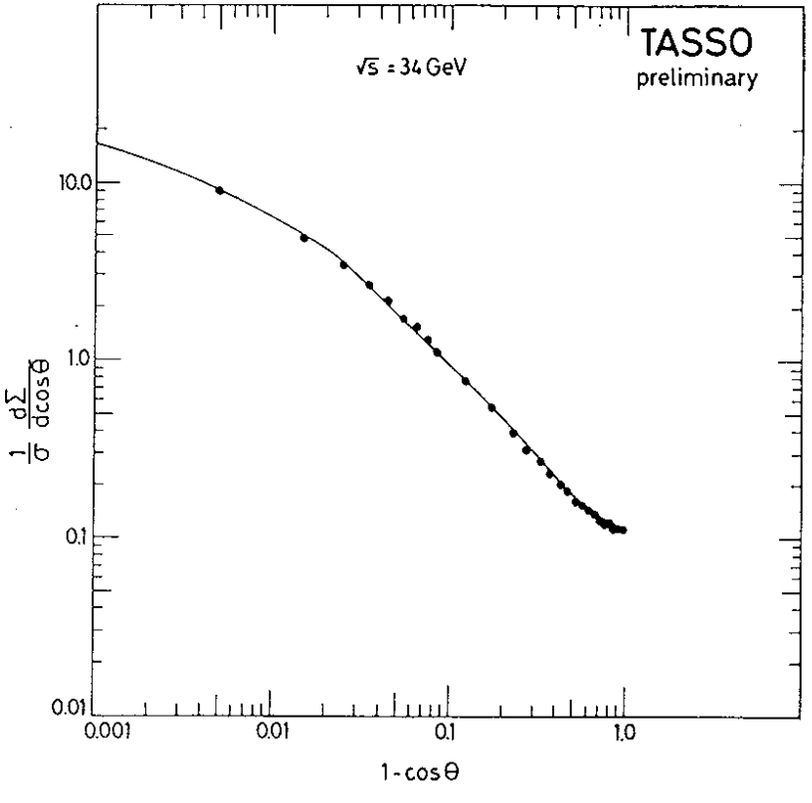
TASSO
preliminary
√s = 34 GeV
10.0
1.0
0.1
0.01
0.001
0.01
0.1
1.0
1 - cos Θ
1/σ dΣ/d cos Θ

Fig. 18

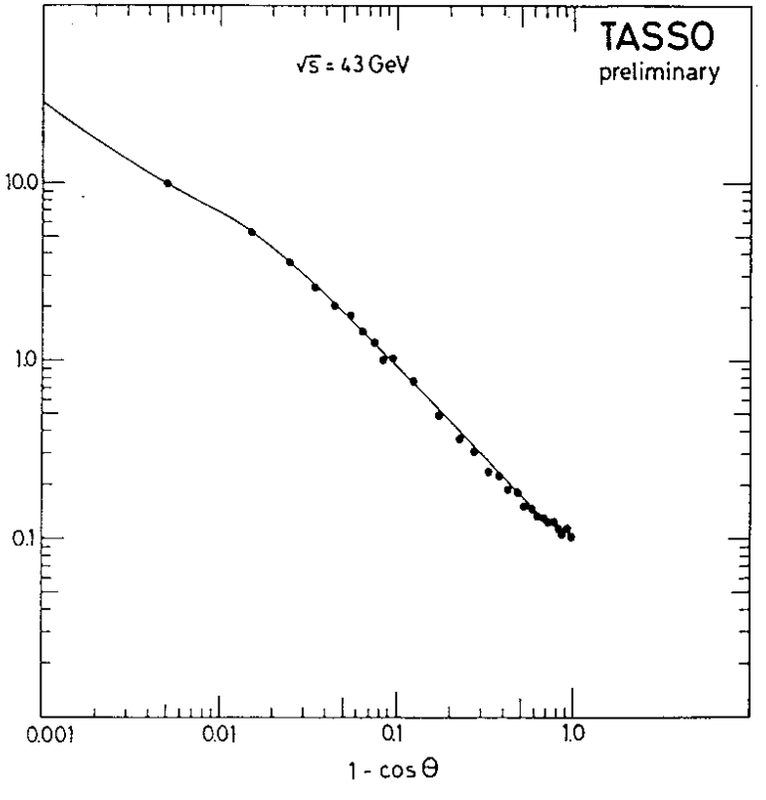
TASSO
preliminary
√s = 43 GeV
10.0
1.0
0.1
0.001
0.01
0.1
1.0
1 - cos Θ

Fig. 19